

Opinion piece



Cite this article: Harris KM, Kuwajima M, Flores JC, Zito K. 2024 Synapse-specific structural plasticity that protects and refines local circuits during LTP and LTD. *Phil. Trans. R. Soc. B* **379**: 20230224.
<https://doi.org/10.1098/rstb.2023.0224>

Received: 17 October 2023
Accepted: 5 January 2024

One contribution of 26 to a discussion meeting issue ‘Long-term potentiation: 50 years on’.

Subject Areas:
neuroscience

Keywords:
synapse, long-term potentiation, ultrastructure, long-term depression, spaced learning

Author for correspondence:
Kristen M. Harris
e-mail: kharris@utexas.edu

Synapse-specific structural plasticity that protects and refines local circuits during LTP and LTD

Kristen M. Harris¹, Masaaki Kuwajima¹, Juan C. Flores² and Karen Zito²

¹Department of Neuroscience and Center for Learning and Memory, The University of Texas at Austin, Austin, TX 78712, USA
²Center for Neuroscience, University of California, Davis, CA 95618, USA

ORCID KMH, 0000-0002-1943-4744; MK, 0000-0002-1478-3726; JCF, 0000-0003-3957-8670; KZ, 0000-0002-0799-0460

Synapses form trillions of connections in the brain. Long-term potentiation (LTP) and long-term depression (LTD) are cellular mechanisms vital for learning that modify the strength and structure of synapses. Three-dimensional reconstruction from serial section electron microscopy reveals three distinct pre- to post-synaptic arrangements: strong active zones (AZs) with tightly docked vesicles, weak AZs with loose or non-docked vesicles, and nascent zones (NZs) with a postsynaptic density but no presynaptic vesicles. Importantly, LTP can be temporarily saturated preventing further increases in synaptic strength. At the onset of LTP, vesicles are recruited to NZs, converting them to AZs. During recovery of LTP from saturation (1–4 h), new NZs form, especially on spines where AZs are most enlarged by LTP. Sentinel spines contain smooth endoplasmic reticulum (SER), have the largest synapses and form clusters with smaller spines lacking SER after LTP recovers. We propose a model whereby NZ plasticity provides synapse-specific AZ expansion during LTP and loss of weak AZs that drive synapse shrinkage during LTD. Spine clusters become functionally engaged during LTP or disassembled during LTD. Saturation of LTP or LTD probably acts to protect recently formed memories from ongoing plasticity and may account for the advantage of spaced over massed learning.

This article is part of a discussion meeting issue ‘Long-term potentiation: 50 years on’.

1. Introduction

Since the discovery of dendritic spines and synapses, changes in their structure and function have been proposed as the neural basis for learning and memory [1–3]. Synaptic plasticity comprises changes in the synapse size and molecular composition that result in the strengthening or weakening of synapses. Long-term potentiation (LTP) and long-term depression (LTD) are cellular mechanisms of learning and memory that modify spine and synapse function, structure and composition [4–14]. Interestingly, when LTP is induced on one part of a neuron, LTD can occur elsewhere, providing a cell-wide homeostasis that averts excess excitation and seizures [15–22]. The LTP-induced synapse enlargement is counterbalanced by shrinkage or stalled outgrowth of distant spines on the same neuron [23,24]. Thus, LTP and LTD could orchestrate memory formation and refinement by coordinating synaptic efficacy via strengthening some synapses while weakening or eliminating others. Retaining the specificity of new memories in the face of ongoing plasticity requires a period of time when recently potentiated synapses are temporarily unavailable for more potentiation [25–28]. Indeed, spaced or

distributed learning produces longer-lasting memories than massed episodes of learning [29–32].

Structural synaptic plasticity is an essential feature of learning, LTP and LTD in the hippocampus [33–35]. While most neuroscientists agree that synaptic structural changes are vital for learning and memory, the cellular and molecular mechanisms that protect recent synaptic changes from being overwritten by ongoing plasticity remain ill-defined. A rich literature describes the importance of trafficking glutamate receptors to and from synapses during LTP, LTD, homeostasis, learning and memory [36–42]. Nanodomains are hypothesized to comprise postsynaptic slots where glutamate receptors could be inserted or removed [43–45]. Nanocolumns form in these domains between postsynaptic glutamate receptors in complex with adhesion molecules that bind to partner adhesion molecules emanating from presynaptic vesicle docking sites [46–48]. Here, we explore changes in the positions of presynaptic vesicles that could underlie the saturation and recovery of the capacity for LTP and LTD and propose models that are consistent with the structural findings.

2. Evidence for the saturation and recovery of LTP in hippocampus

Several independent studies have established that induction of LTP temporarily inhibits the induction of further LTP for a period of time. For example, theta-burst stimulation (TBS) delivered at half-maximal response saturates LTP (figure 1) [24,49–53]. In the hippocampus of adult Long–Evans hooded rats at 30 or 60 min after saturation, no additional LTP can be induced (figure 1*a*). About 20% of slices recover from saturation and exhibit more LTP by 90 min, 50% by 120 min and 80% by 180 min, and reliable recovery occurs by 4 h (figure 1*b,c*) [49]. Induction of LTP after recovery from saturation is blocked by 2-amino-5-phosphonopentanoic acid (APV) (figure 1*c*), supporting that the recovered LTP was induced by the same *N*-methyl-D-aspartate receptor (NMDAR)-dependent mechanisms as the initially saturated LTP [49].

3. Evidence that synapse enlargement during recovery of LTP is silent

In order to pinpoint the origin of LTP saturation, the effect of LTP induction on synaptic ultrastructure has been investigated. Synaptic structure was evaluated in slices fixed after LTP was induced at one electrode and control pulses received at another electrode located greater than 500 μm away to ensure independence of control and LTP synapse populations (figure 2*a*). Serial sections were obtained at approximately 120 μm from the TBS and control stimulating electrodes. Dendrites were imaged and synapses were reconstructed through serial section electron microscopy (figure 2*b,c*). Synapses reconstructed along dendrites from control and LTP conditions revealed the time-lapse sequence of structural synaptic plasticity (figure 2*d*). At 5 or 30 min after induction, the average postsynaptic density (PSD) area on individual spines was unchanged despite maximal potentiation. By 2 h, the total PSD area was increased relative to all other times and conditions, and to perfusion-fixed hippocampus *in vivo* [24,54]. This effect was greatest in dendritic regions of high spine density, namely, spine clusters, as discussed further below. The PSD enlargement at 2 h occurred without additional potentiation and thus was effectively silent.

4. Evidence that nascent zone plasticity contributes to the timing and specificity of LTP

Our studies have identified that the induction of LTP is accompanied by the filling of presynaptic nascent zones (NZs). Three-dimensional reconstruction from serial section electron microscopy (3DEM) distinguishes active zones (AZs) from NZs (figure 3*a–e*) [50]. AZs have docked, non-docked and reserved pool presynaptic vesicles, whereas we delineate NZs as comprising a well-defined PSD but lacking presynaptic vesicles. The PSD of the NZ is morphologically indistinguishable from the PSD located directly beneath the AZ. NZs are rich in scaffolding proteins containing open slots where glutamate receptors can insert and where interaction with and stabilization of postsynaptic receptors and adhesion molecules leads to new trans-synaptic nanocolumns [39,43,55–57].

The growth of NZs accompanies the functionally silent growth of the PSD (figure 3*f–l*). By 5 min after induction of LTP, small dense core vesicles (DCVs), tethered with a cluster of synaptic vesicles, are recruited to presynaptic boutons (figure 3*f,g*). The tethering filaments comprise presynaptic scaffolding proteins, and the dense core contains cell adhesion molecules [58,59]. Thus, the fusion of DCVs with the presynaptic membranes puts core adhesion molecules in the synaptic cleft, where they can bind with postsynaptic receptors and stabilize them in a nanocolumn where they respond to subsequent release of neurotransmitter. The surface of a single DCV and its tethered vesicles is sufficient to fill a whole NZ and convert it to an AZ (figure 3*h,i*). At 5 min, the relative frequency of NZs in control and LTP conditions has not changed. By 30 min, NZs diminish as AZs enlarge, while the average whole PSD area remains unchanged (figure 3*j*, see figure 2*d*). By 2 h, NZ enlargement accounts for most of the PSD enlargement (figure 3*k*). Furthermore, the synapses that underwent the most AZ enlargement were also the synapses that re-acquired NZ (figure 3*l*). These findings suggest that the filling of NZ saturates LTP and that the regrowth of NZs underlies the recovery of the capacity for subsequent LTP, especially at the most enlarged synapses.

5. Effects of LTP on strong versus weak active zones as defined by presynaptic vesicle positions

In addition to the filling of NZs, LTP induction results in the conversion of weak AZs to mature AZs. EM tomography reveals precise positions of docked presynaptic vesicles [60,61]. These vesicles have filamentous tethers to the AZ composed of molecules involved in docking, priming and release. The position of vesicles at the AZ varies with functional status. Tightly docked vesicles touch the presynaptic membrane (figure 4*a–f*) and are primed for the release of neurotransmitter. Loosely docked vesicles (less than 8 nm) and non-docked vesicles (greater than 8 nm) comprise recycling and reserve pools (figure 4*g–j*). The density of tightly docked vesicles is increased during LTP, but loose or non-docked vesicle densities are unchanged (figure

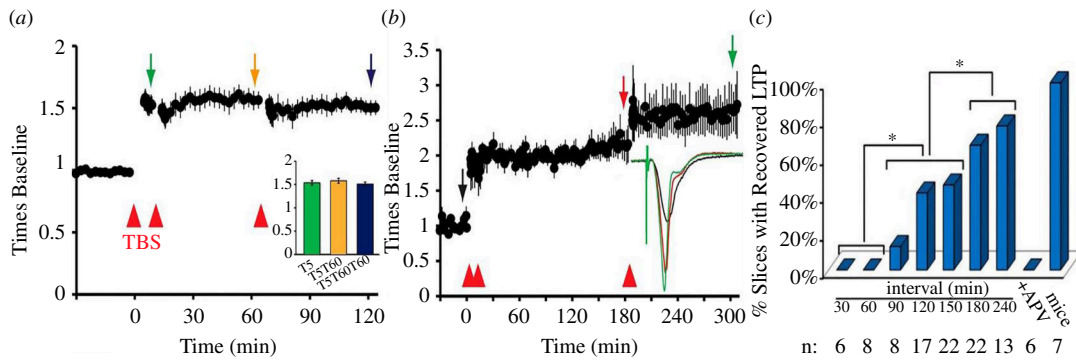


Figure 1. Saturation and recovery of LTP in stratum radiatum of hippocampal CA1 from adult rats. (a) The first two bouts of theta-burst stimulation (1 TBS = 8 trains at 30 s intervals of 10 bursts at 5 Hz with 4 pulses/burst at 100 Hz, delivered at approximately half-maximal response of the field excitatory postsynaptic potential (fEPSP) determined prior to baseline stimulation, red arrowheads) demonstrate saturation of LTP that lasts for at least 60 min (yellow and blue bars, eight slices with error bars). (b) LTP recovery at 180 min (22 slices with error bars). (c) Timing of the recovery of LTP in rat and mouse hippocampal slices (n = number of slices). Adapted from [49].

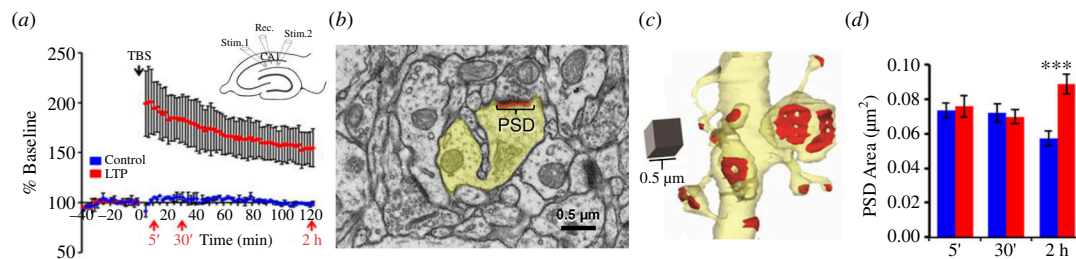


Figure 2. Evidence that synapse enlargement is silent during the recovery of capacity for LTP. (a) LTP demonstrated from within-slice experiments. In separate experiments, the slices were fixed at 5 min, 30 min or 2 h after the induction of LTP. (Inset shows electrode positions in CA1, stratum radiatum of an acute slice. TBS was delivered to Stim. 1 or Stim. 2, to counterbalance for distance from area CA3. The tissue was sampled in the vicinity of the two stimulating electrodes to obtain synapses that underwent TBS and induction of LTP versus control stimulation in the same slice.) (b) Electron microscopy image illustrating a dendrite (yellow) and postsynaptic density (PSD, red). (c) Three-dimensional reconstruction of dendrite (yellow) with PSD areas (red) in a region of high spine density. (d) PSD sizes in the LTP and control conditions when fixed at 5 min, 30 min or 2 h after the induction of LTP. PSDs were enlarged at 2 h relative to all other conditions ($p < 0.001$). Control PSD area is on average smaller by 2 h as new small spines emerged during control stimulation. This small spine outgrowth was stalled in favour of PSD enlargement during LTP. (Adapted from [24,50].)

4k). The tethering filaments are shorter for both tight and loose docked vesicles after LTP (figure 4l–p), supporting that more vesicles are stabilized in the docked and primed state by 2 h during LTP [60].

6. Relationship of strong versus weak active zones to glutamate response profiles

Synaptic modelling suggests that the conversion of weak AZs to mature AZs is accompanied by synaptic strengthening. MCell is a particle-based Monte Carlo simulator of biochemical reactions and diffusion that has been used to predict the number of open α -amino-3-hydroxy-5-methyl-4-isoxazolepropionic acid receptor (AMPA) with distance from a vesicle release site (figure 5a,b) [63–69]. The MCell model allows AMPARs to diffuse freely and form nanodomains of approx. 20–30 receptors [46]. Modelling based on experimental evidence shows that the probability of activating an AMPAR is only 0.4 beneath a release site and falls off precipitously within 100 nm from the release site [62,63,70–72]. Thus, the response of AMPARs in nanodomains of the AZ would be greatest where docked presynaptic vesicles are clustered [61,73–75].

The distance from docked vesicles to the NZ increases with LTP (figure 5c), further emphasizing the likelihood that the NZ growth is silent during LTP, even if an AMPAR were to enter the NZ [62,71]. Thus, by these definitions, a strong AMPAR response zone would constitute a 100 nm region surrounding the centre of docked vesicles, whereas weak AMPAR response zones would be located beneath loose and non-docked vesicles [76–79]. NZs would be unlikely to have strong or weak AMPAR response zones based on the absence of docked, loose or non-docked vesicles in them (figure 5g).

7. Molecular mechanisms underlying conversion of NZs to AZs at potentiated synapses

The cellular and molecular mechanisms that drive coordinated changes in pre- and post-synaptic structure and molecular content during the saturation and recovery of LTP are not yet well defined. However, there are many clues in the literature that give rise to a plausible sequence of events that we have outlined in figure 6. AZs contain filled AMPAR slots bound to neuroligin via the PSD scaffolding proteins and to neuroligin on the presynaptic side, thus positioning AMPARs directly beneath presynaptic release sites (figure 6a). We propose that NZs contain empty AMPAR slots that are bound to neuroligin and protected from non-specific capture of AMPAR, possibly by SynGAP, a GTPase-activating protein (figure 6a) [80]. Other cell adhesion molecules that have been shown to be involved in LTP are located adjacent to the NZ at the perimeter of the synapse [81–86]. Extrasynaptic AMPARs are located outside the NZ and AZ and are highly mobile in the spine membrane.

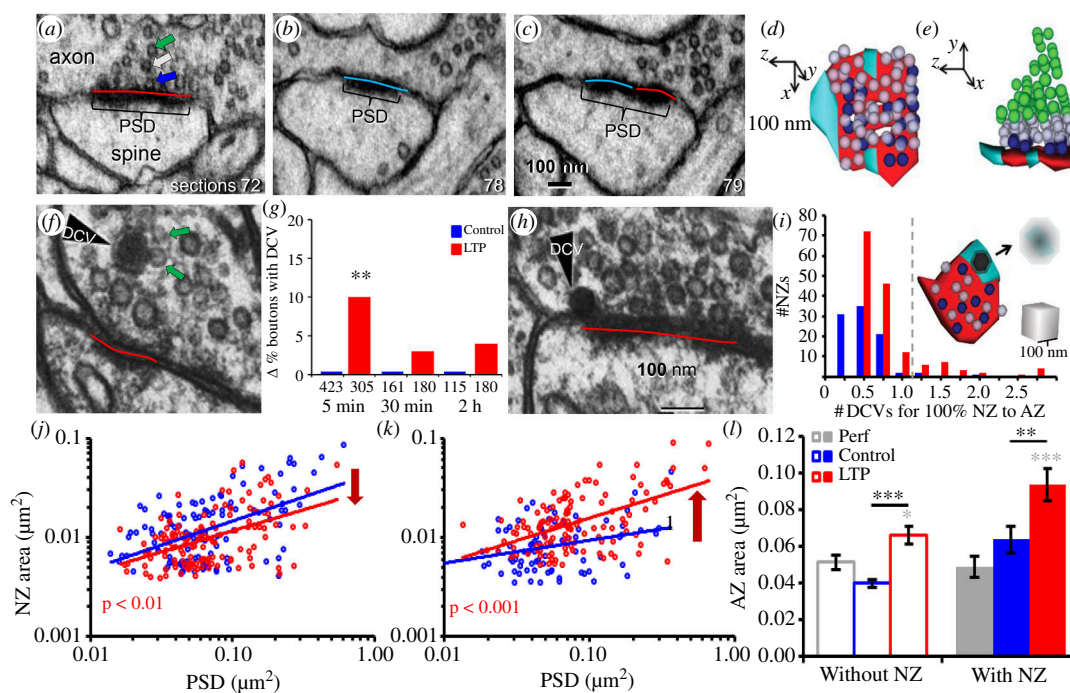


Figure 3. Evidence that nascent zone plasticity mediates the saturation and recovery of LTP. (a) Active zone (red) with docked (royal blue arrow), non-docked (white arrow), and reserve (green arrow) vesicles, and a PSD. (b, c) Nascent zone (aqua) has a PSD but no presynaptic vesicles above it. (d, e) Three-dimensional reconstructions of the synapse illustrated in a–c. (f) Electron microscopy (EM) image illustrating synaptic vesicles that are tethered (green arrows) to a dense core vesicle (DCV). (g) DCVs are recruited from inter-bouton regions to synaptic boutons at 5 min after TBS (n = number of syn). (h) DCV at the edge of an AZ. (i) Plot of the number of DCVs that would be needed to convert a NZ to AZ by filling it with the tethered docked vesicles versus the number of NZs in the control or LTP conditions that would be fully converted to AZ if a DCV were to be recruited with tethered vesicles. (j) NZ area decreases by 30 min after LTP induction. (k) NZ size is re-elevated by 2 h after LTP induction. (l) NZ recovery at 2 h during LTP is greatest on spines with the largest AZ areas (Perf = *in vivo* controls). (Adapted from [50].)

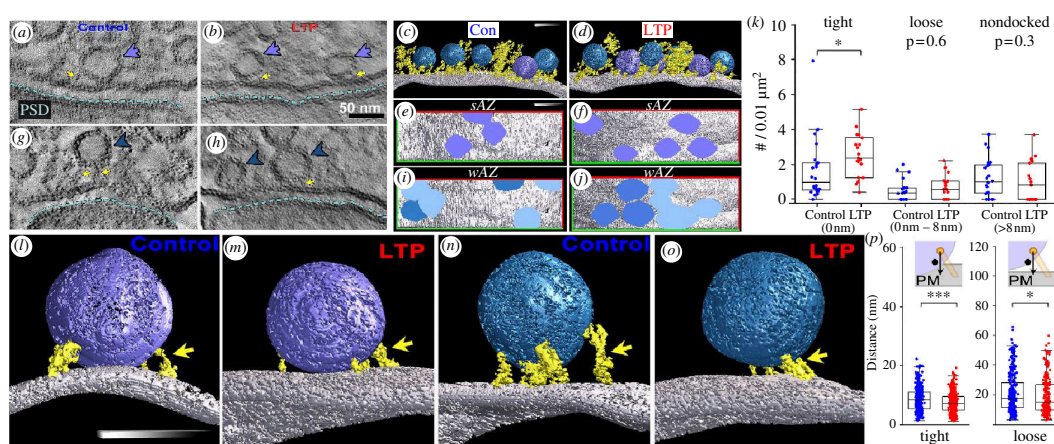


Figure 4. Effects of LTP on strong versus weak active zones defined by the positioning of presynaptic vesicles. (a–f) Strong active zones (sAZ) have tightly docked vesicles (purple). (g–j) Weak active zones (wAZ) have loosely docked (turquoise) or non-docked (light blue) vesicles. (Molecular tethering filaments are illustrated in yellow). (c, d) Side view of three-dimensional tomogram illustrates presynaptic membrane surface (silver) with tight and loose docked vesicles and tethering filaments. Unbiased sampling frames for (e, f) tight and (i, j) loose or non-docked vesicles. (k) The density of tightly docked vesicles, but not loose or non-docked vesicles, increases in the tomographic nanodomains after LTP. (l–p) The length of the tethering filaments for both tight and loose docked vesicles was shortened at 2 h after LTP induction. (Adapted from [60].)

Upon induction of LTP, the slot protector is released from empty slots in the PSD (figure 6b) [80]. A pressure-sensitive signal is transduced as the spine enlarges, resulting in the aggregation of soluble N-ethylmaleimide fusion protein attachment protein receptor (SNARE) proteins at new presynaptic release sites (figure 6b) [86,87]. DCVs release their contents, including neurexin, which binds to neuroligin (figure 6b) [62,71]. Mobile AMPARs are then trapped in the slot beneath the newly formed presynaptic AZ (figure 6c). These events happen within the first 30 min after the induction of LTP and are consistent with prior studies on the mobility and capture of AMPAR to form new nanocolumns [39,47,88–91]. With time, new NZs are formed, containing new slots for the capture of mobile AMPAR, and thus, LTP recovers from saturation (figure 6d). This model is an extension of the slot model originally proposed by Lisman & Raghavachari [43]. Notably, our expanded model significantly differs in relative positioning of presynaptic vesicles before the induction of LTP. Although alternative mechanisms are possible, we have chosen to highlight in our model novel mechanisms that have been discovered since the original model was proposed.

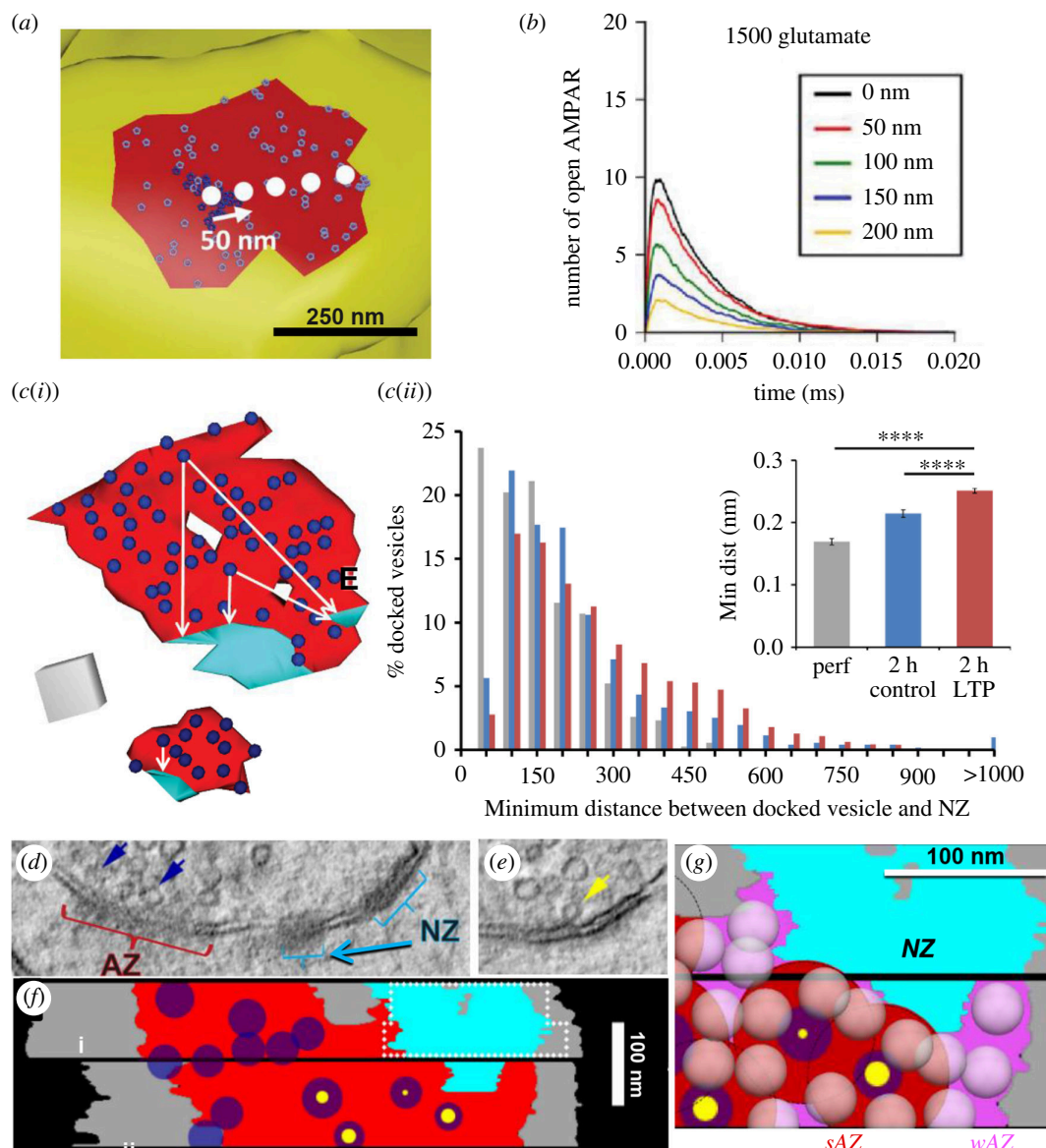


Figure 5. Relationship of strong versus weak AZ to AMPAR open response profiles and the effects of LTP on docked vesicle positions relative to nascent zones. (a) Simulated glutamate release sites (white circles), stable (dark blue) and mobile (light blue) AMPARs across a PSD surface (red). (b) MCell model reveals a decrease in AMPAR activation with distance from release sites. (c(i)) The minimum distance from a docked vesicle to a nascent zone (c(ii)) increases from 200 nm in control to 250 nm by 2 h of LTP. (d) Dual-axis tilt tomography reveals docked vesicles (navy arrows) and (e) a vesicle making an omega figure resulting in a pore (yellow arrow). (f) Reconstruction through two serial sections (approx. 100 nm each) of an axon-spine interface (grey), with docked vesicles (blue) and pores scaled by opening size (yellow). (Virtual section thickness = 3 nm.) (g) In tomograms, strong active zones (sAZ) encompass regions with less than 50% drop in receptor response (100 nm) around vesicle docking sites. Weak AZs (wAZ) only have loose or non-docked vesicles (white translucent) that are in a position where they could eventually dock. NZs (turquoise) have no presynaptic vesicles. (a and b are adapted from [62] and c–g are adapted from [50].)

8. Effects of LTP resources that enable synapse enlargement and spine clustering

The largest synapses occur on dendritic spines that contain smooth endoplasmic reticulum (SER) (figure 7a–d). These SER-containing spines are referred to as ‘sentinel spines’ because small spines cluster around them [54]. SER is a highly motile organelle that regulates calcium and local trafficking of lipids and proteins and provides a site for post-translational modification of proteins [92–94]. SER is a limited resource, entering less than 15% of hippocampal CA1 spines [54,95,96]. By 2 h after the induction of LTP, the type of SER contained in spines shifts from a single tubule under control conditions to a fully elaborated spine apparatus with LTP (figure 7c). Spines containing SER undergo substantial PSD enlargement during LTP (figure 7d). Most synapses in hippocampal area CA1 occur on dendritic spines that contain no SER (figure 7e), and LTP has only a small effect on the PSD area of spines lacking SER (figure 7f). Polyribosomes (PRs) have three or more ribosomes that form when mRNAs are unmasked and made available for local protein synthesis (figure 7g) [97–100]. PRs indicate locations where the synthesis of multiple copies of synaptic proteins occurs and where local circuits are enhanced, protected or refined during the saturation and recovery of LTP, learning and memory [101–105]. During LTP, PSDs on spines with polyribosomes undergo some enlargement that is greater than on spines without SER, but less than on spines with SER (figure 7h) [54,106].

Dendritic spines are more likely to cluster in the vicinity of a large sentinel spine that contains SER than in the neighbourhood of spines lacking SER (figure 7i) [24,50,54]. Where the SER in the dendritic shaft branches or expands, trafficking slows and ER exit sites deliver resources locally to support synapses in the clusters [94]. High-density spine clusters are longer and

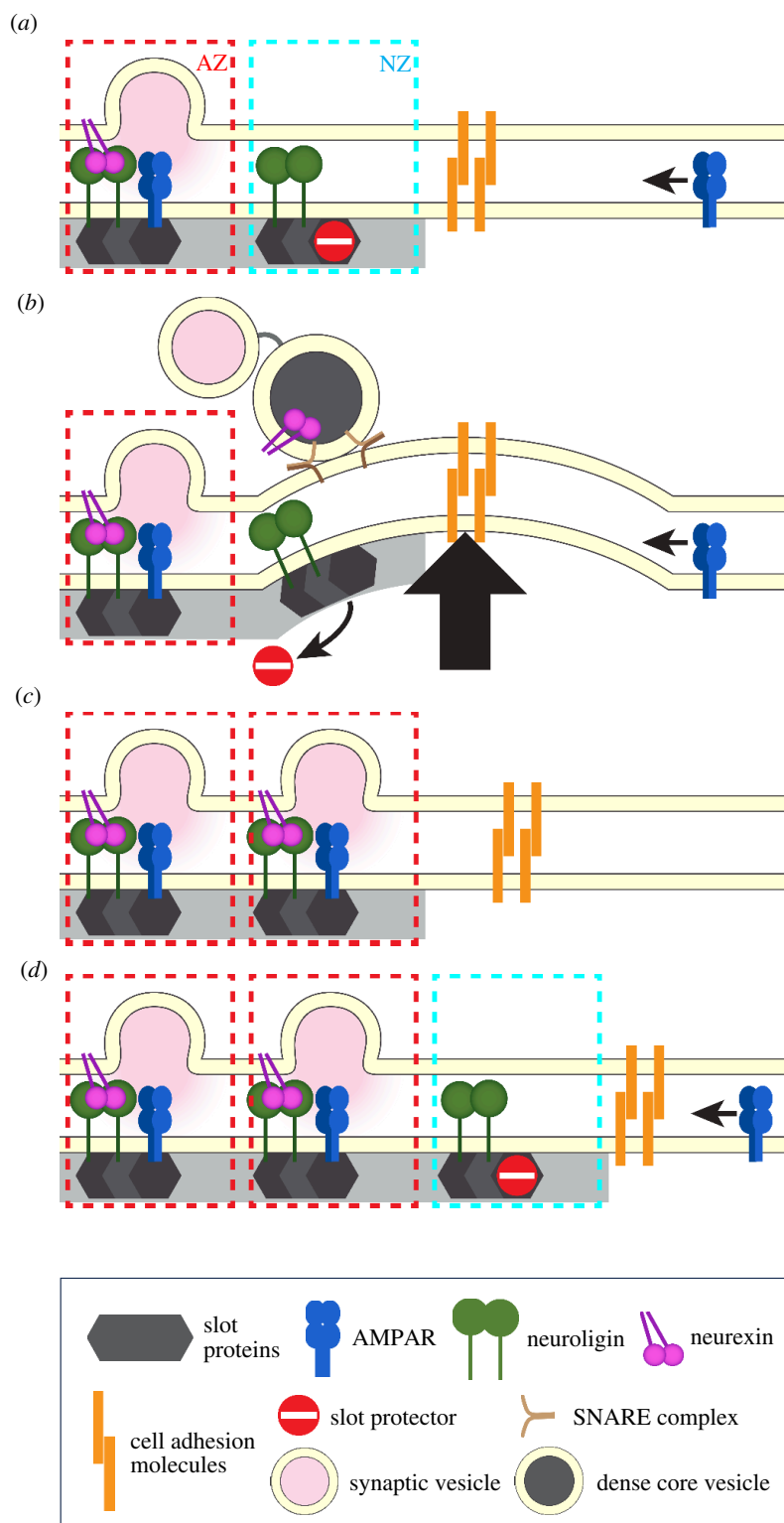


Figure 6. Molecular mechanisms of NZ to AZ plasticity. (a) Starting synapse with active (AZ) and nascent (NZ) zones. (b) LTP is induced, the spine enlarges (large black arrow), and a series of events are triggered resulting in (c) the capture of AMPAR to the previous NZ and the formation of a new AZ. (d) With time, a new NZ is created. See text for detailed descriptions.

have more SER branches than low-density clusters (figure 7*i,j*). Following LTP, the density of spines in a cluster that contains a sentinel spine remains high, and the total synapse area is elevated as these synapses enlarge (figure 7*k*). In contrast, spine density in a cluster lacking sentinel spines remains low or is further reduced following LTP (figure 7*l*). In addition, fewer SER branches remain in the high-density clusters around sentinel spines after LTP (figure 7*m*), possibly reflecting the consumption of SER to support PSD growth and elaboration of the spine apparatus. This SER consumption may also contribute to the saturation of LTP, and recovery might require SER to elaborate in the shaft or spines of the cluster to ready it for subsequent recovery of LTP.

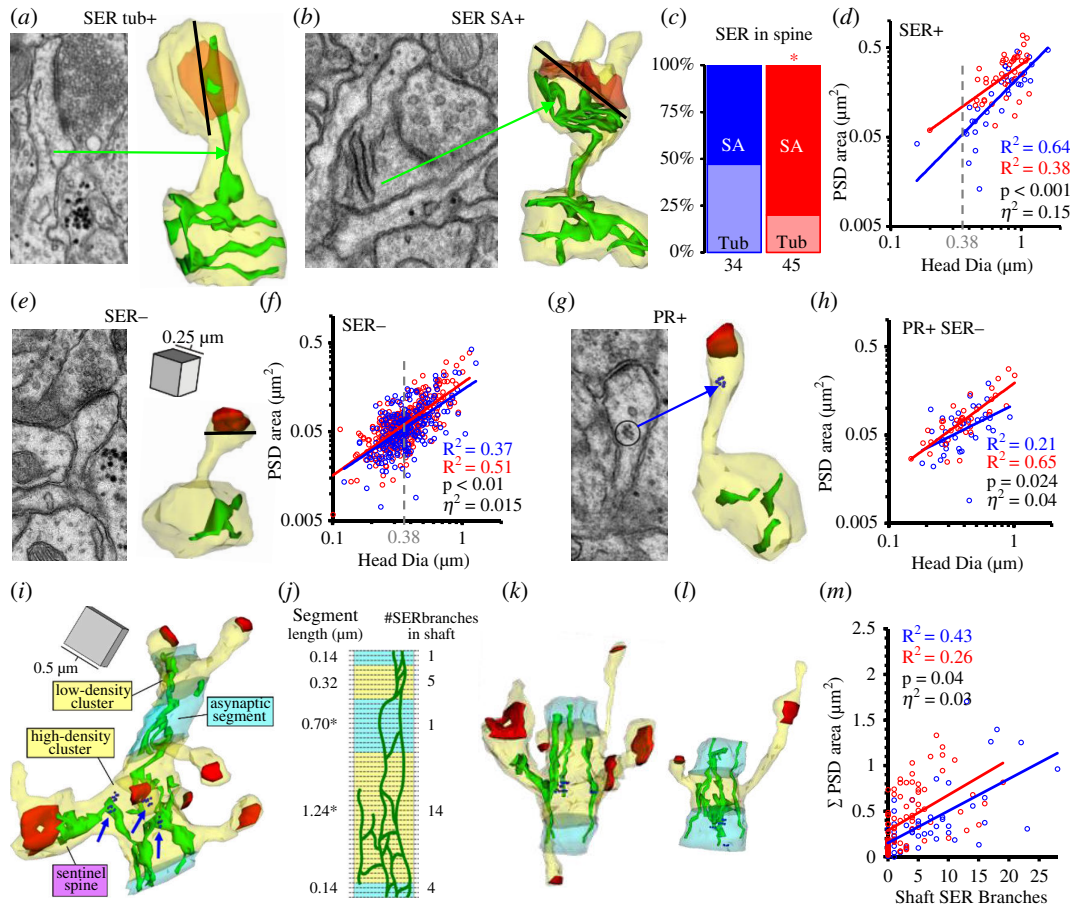


Figure 7. Effects of LTP on sentinel spines and dendritic resources that enable maximum synapse enlargement and spine clustering. (a) EM image and three-dimensional reconstruction of a 2 h control spine containing a tubule (tub) of SER (green). (b) EM image and three-dimensional reconstruction of a 2 h LTP spine containing a spine apparatus (SA). (c) About 12% of control spines have SER, distributed 50:50 between single tubules and spine apparatus, whereas by 2 h after the induction of LTP, the same frequency of spines contain SER, but more than 80% of them have an elaborate spine apparatus (SA). (d) Enlargement of PSDs on SER-containing spines following LTP. (e) EM image and three-dimensional reconstruction of spine without SER. (f) PSD enlargement on SER- spines following LTP. (g) EM image and three-dimensional reconstruction of a spine containing a polyribosome (PR). (h) PSD enlargement on PR containing spines following LTP. (i) Delineating spine clusters: sentinel, SER-containing, spine, in a high-density cluster contrasting with low-density cluster. (j) Quantifying SER branches in the dendritic shafts. (k) High-density spine cluster in the 2 h LTP condition. (l) Low-density spine cluster in the 2 h control condition. (m) Relationship between summed PSD area across spines in clusters versus shaft SER branches increases following LTP. (Adapted from [54].)

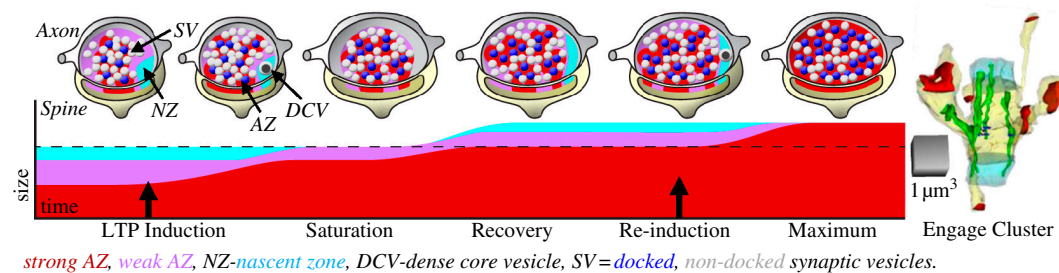


Figure 8. Model of structural synaptic plasticity during the saturation and recovery of LTP.

9. Modelling AZ and NZ plasticity and spine clustering during saturation and recovery of LTP

Our model of structural synaptic plasticity that accompanies LTP accounts for the timing of the stages of saturation and recovery during LTP (figure 8) [19,45,107–109]. At the start, synapses have strong AZs with docked vesicles forming nanodomains with postsynaptic receptors, weak AZs with loosely tethered or non-docked presynaptic vesicles, and silent NZs. Within minutes of induction, DCVs with tethered presynaptic vesicles are recruited to the NZs where they dock and convert NZs to AZs, and LTP becomes saturated [50,60,61]. With time, new NZs are added and the capacity for LTP recovers. Ultimately, the capacity for LTP at one synapse reaches a maximum, limited by synapse size and resources. Once a synapse reaches maximal strength on a sentinel spine, continued strengthening of a local synaptic circuit would be achieved by engaging neighbouring spines to form stronger, more effective synaptic clusters to overcome the limit and result in stronger spine clusters [54,85,110–115]. Indeed, under some circumstances, new spines emerge near other spines to form clusters during LTP and learning [110,116–128].

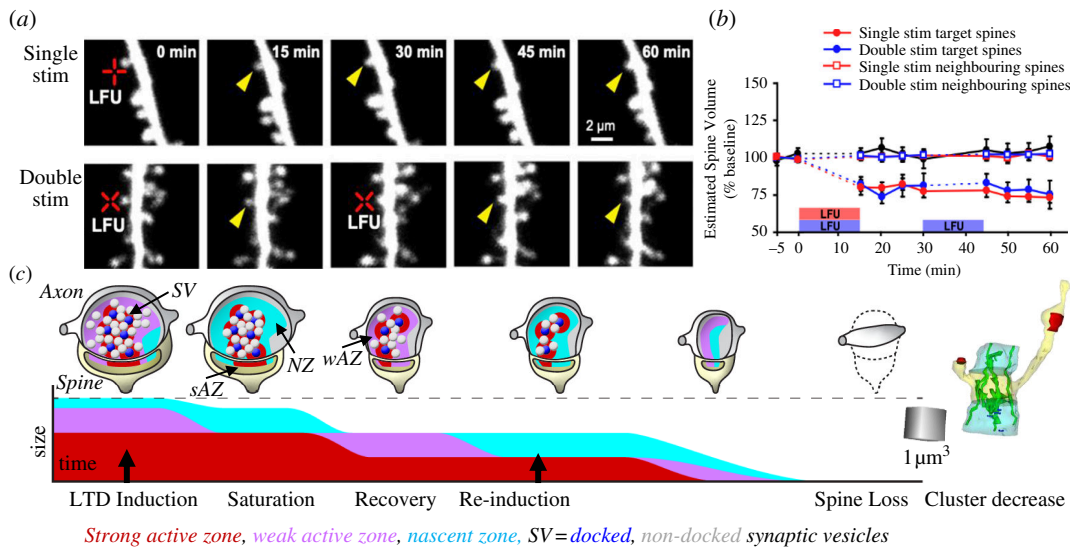


Figure 9. Synaptic plasticity during saturation and recovery of the capacity for LTD. (a) Two-photon imaging of LTD-associated dendritic spine shrinkage induced by low-frequency glutamate uncaging (LFU; 90 pulses of 0.2 mS at 0.1 Hz, adapted from [136]). (b) Demonstration of the saturation of LTD-associated dendritic spine shrinkage: a second LFU fails to induce further spine shrinkage. (c) Model of LTD involving weak active zones, strong active zones, nascent zones and loss of dendritic spines that results in low-density spine clusters or no spine clustering.

Multiple postsynaptic mechanisms could mediate the recruitment of neighbours during LTP. In one such mechanism, the SER could enable calcium signalling that propagates from the sentinel spine to the neighbouring spines via calcium-induced calcium release from stores. Alternatively, the SER could generate lipids both for creating the spine apparatus and for enlarging neighbouring spines. Notably, SER with ribosomes forming rough endoplasmic reticulum has been observed in some spines and could provide local synthesis of membrane-spanning proteins such as AMPARs. Where the SER branches or forms a spine apparatus, vesicles of Golgi outposts can be generated that deliver newly synthesized membrane-spanning proteins to the surface. Retrograde signalling could also play a role in the recruitment of neighbouring spines during LTP saturation and recovery. Presynaptic axons associated with other spines in the cluster would be primed for subsequent plasticity via the spread of a retrograde signal, such as nitric oxide, making those axons more ready to engage in subsequent bouts of LTP [85,113–115,129].

This model provides a solid framework to understand the specificity of synaptic plasticity and the local limits defining structural mechanisms of LTP. Testing this model could serve as the basis of future work on synaptic plasticity in various animal models that reveal the formation of memory engrams or disrupt learning, memory and behaviour [27,28,51,130–134].

10. Modelling the saturation and recovery of LTD and its impact on structural synaptic plasticity

It is an important consideration whether similar mechanisms of saturation of plasticity are at play during LTD of synaptic strength. Notably, there is strong evidence in the literature that physiological LTD and LTD-associated spine shrinkage also saturate [135–137]. Indeed, full saturation of LTD-associated spine shrinkage occurs 30 min post-LTD induction by low-frequency glutamate uncaging at individual dendritic spines (figure 9a,b) [136]. Because LTD was induced in these experiments using a low-frequency glutamate uncaging (LFU) [136,138], the induction of LTD and associated spine shrinkage bypasses presynaptic stimulation and produces a spine-specific coordinated decrease in size and synapse strength. These findings suggest that LTD saturation originates postsynaptically and is transmitted back to the presynaptic side through retrograde messengers, bidirectional adhesive signalling or direct physical forces, as described for LTP above.

Based upon the dynamics and morphology of weak AZs (figure 4) [60], we propose a model in which LTD weakens synapses and circuits by removal of weak AZs, which are less stable than strong AZs. Loss and endocytosis of AMPARs that become untethered leads to the loss of slots and presynaptic vesicle docking sites, and ultimately the disassembling of nanocolumns (figure 9c) [139–144]. Saturation of LTD would occur when all weak AZs are either converted to NZs or eliminated. Based on the localization of weak AZs, we predict that the edges of the AZ are less stable than those located in the middle of an AZ. We hypothesize that saturation will be released over time, and the capacity for additional LTD will recover as strong AZ are weakened at their edges, thereby providing new weak AZ areas for disassembly. As this process continues, dendritic spines will shrink, ultimately leading to spine loss and reduced cluster strength [145]. Future experiments will test this model through examining the ultrastructural changes that accompany the saturation and recovery of LTD.

11. Summary

Evidence for the saturation and recovery of LTP and LTD via AZ and NZ plasticity is presented. Mechanistic and structural models of this plasticity account for the time delays between saturation and recovery. Local spine clustering would provide

specificity while engaging spines in the neighbourhood of a large sentinel spine by sharing local resources, such as SER and ribosomes postsynaptically and retrograde signalling to their presynaptic axons. This plasticity would provide a synaptic mechanism for the advantage of spaced-over massed learning. New tools are under development to speed and refine the analyses so that future work could test whether NZ plasticity coincides with spaced learning and associated behaviours. Testing these models will provide new insights into synaptic plasticity mechanisms that protect and refine local circuits as a basis of learning and memory and towards new targets for understanding and treating cognitive dysfunction.

Ethics. This work did not require ethical approval from a human subject or animal welfare committee.

Data accessibility. This article has no additional data.

Declaration of AI use. We have not used AI-assisted technologies in creating this article.

Authors' contributions. K.M.H.: conceptualization, data curation, formal analysis, funding acquisition, investigation, methodology, project administration, resources, supervision, validation, visualization, writing—original draft, writing—review and editing; M.K.: conceptualization, visualization, writing—review and editing; J.C.F.: conceptualization; K.Z.: conceptualization, writing—review and editing.

All authors gave final approval for publication and agreed to be held accountable for the work performed therein.

Conflict of interest declaration. We declare we have no competing interests.

Funding. This research was supported by National Institute of Mental Health (R01MH095980) the National Institute for Neurological Disorders & Stroke (R01NS06736) and Division of Biological Infrastructure (NSF NCS-FO: 2219894).

References

- Ramón Y Y, Cajal S. 1891 Sur la structure de l'écorce cerebrale de quelques mammiferes. *Cellule* **7**, 124–176.
- Ramón Y, Cajal S. 1896 Las espinas colaterales de las celulas del cerebro tenidas por el azul de metileno. *Revista Trimestral Micrografica* **1**, 123–136.
- Kasai H, Ziv NE, Okazaki H, Yagishita S, Toyozumi T. 2021 Spine dynamics in the brain, mental disorders and artificial neural networks. *Nat. Rev. Neurosci.* **22**, 407–422. (doi:10.1038/s41583-021-00467-3)
- Bliss TV, Lomo T. 1973 Long-lasting potentiation of synaptic transmission in the dentate area of the anaesthetized rabbit following stimulation of the perforant path. *J. Physiol.* **232**, 331–356. (doi:10.1113/jphysiol.1973.sp010273)
- Lynch G, Kessler M, Arai A, Larson J. 1990 The nature and causes of hippocampal long-term potentiation. *Prog. Brain Res.* **83**, 233–250. (doi:10.1016/s0079-6123(08)61253-4)
- Bliss TVP, Collingridge GL, Morris RGM. 2003 Long-term potentiation: enhancing neuroscience for 30 years. *Phil. Trans. R. Soc. B* **358**, 603–842.
- Bliss TV, Collingridge GL, Morris RG. 2014 Synaptic plasticity in health and disease: introduction and overview. *Phil. Trans. R. Soc. Lond. B* **369**, 20130129. (doi:10.1098/rstb.2013.0129)
- Moreno A. 2021 Molecular mechanisms of forgetting. *Eur. J. Neurosci.* **54**, 6912–6932. (doi:10.1111/ejn.14839)
- Ge Y, Dong Z, Bagot RC, Howland JG, Phillips AG, Wong TP, Wang YT. 2010 Hippocampal long-term depression is required for the consolidation of spatial memory. *Proc. Natl Acad. Sci. USA* **107**, 16 697–16 702. (doi:10.1073/pnas.1008200107)
- Nabavi S, Fox R, Proulx CD, Lin JY, Tsien RY, Malinow R. 2014 Engineering a memory with LTD and LTP. *Nature* **511**, 348–352. (doi:10.1038/nature13294)
- Awasthi A *et al.* 2019 Synaptotagmin-3 drives AMPA receptor endocytosis, depression of synapse strength, and forgetting. *Science* **363**, eaav1483. (doi:10.1126/science.aav1483)
- Kemp A, Manahan-Vaughan D. 2007 Hippocampal long-term depression: master or minion in declarative memory processes? *Trends Neurosci.* **30**, 111–118. (doi:10.1016/j.tins.2007.01.002)
- Saudargiene A, Cobb S, Graham BP. 2015 A computational study on plasticity during theta cycles at Schaffer collateral synapses on CA1 pyramidal cells in the hippocampus. *Hippocampus* **25**, 208–218. (doi:10.1002/hipo.22365)
- Harris KM. 2020 Structural LTP: from synaptogenesis to regulated synapse enlargement and clustering. *Curr. Opin. Neurobiol.* **63**, 189–197. (doi:10.1016/j.conb.2020.04.009)
- Abraham WC. 2003 How long will long-term potentiation last? *Phil. Trans. R. Soc. Lond. B* **358**, 735–744. (doi:10.1098/rstb.2002.1222)
- Abraham WC. 1999 Metaplasticity: key element in memory and learning? *News Physiol. Sci.* **14**, 85. (doi:10.1152/physiologyonline.1999.14.2.85)
- Abraham WC. 1996 Induction of heterosynaptic and homosynaptic LTD in hippocampal sub-regions *in vivo*. *J. Physiol. Paris* **90**, 305–306. (doi:10.1016/s0928-4257(97)87902-8)
- Abraham WC. 2000 Persisting with LTP as a memory mechanism: clues from variations in LTP maintenance. In *Neuronal mechanisms of memory formation: concepts of long-term potentiation and beyond* (ed. C Hölscher), pp. 37–57. Cambridge, UK: Cambridge University Press. (doi:10.1017/CB09780511529818)
- Abraham WC. 2008 Metaplasticity: tuning synapses and networks for plasticity. *Nat. Rev. Neurosci.* **9**, 387. (doi:10.1038/nrn2356)
- Bear MF. 1996 A synaptic basis for memory storage in the cerebral cortex. *Proc. Natl Acad. Sci. USA* **93**, 13 453–13 459. (doi:10.1073/pnas.93.24.13453)
- Bear MF. 1997 How do memories leave their mark? *Nature New Biol.* **385**, 481–482. (doi:10.1038/385481a0)
- Bear MF, Abraham WC. 1996 Long-term depression in hippocampus. *Annu. Rev. Neurosci.* **19**, 437–462. (doi:10.1146/annurev.ne.19.030196.002253)
- Oh WC, Parajuli LK, Zito K. 2015 Heterosynaptic structural plasticity on local dendritic segments of hippocampal CA1 neurons. *Cell Rep.* **10**, 162–169. (doi:10.1016/j.celrep.2014.12.016)
- Bourne JN, Harris KM. 2011 Coordination of size and number of excitatory and inhibitory synapses results in a balanced structural plasticity along mature hippocampal CA1 dendrites during LTP. *Hippocampus* **21**, 354–373. (doi:10.1002/hipo.20768)
- Naqib F, Sossin WS, Farah CA. 2012 Molecular determinants of the spacing effect. *Neural Plast.* **2012**, 581291. (doi:10.1155/2012/581291)
- Naqib F, Farah CA, Pack CC, Sossin WS. 2011 The rates of protein synthesis and degradation account for the differential response of neurons to spaced and massed training protocols. *PLoS Comput. Biol.* **7**, e1002324. (doi:10.1371/journal.pcbi.1002324)
- San Luis CO de, Ryan TJ. 2023 Correction: understanding the physical basis of memory: molecular mechanisms of the engram. *J. Biol. Chem.* **299**, 105070. (doi:10.1016/j.jbc.2023.105070)
- Rao-Ruiz P, Visser E, Mitrić M, Smit AB, van den Oever MC. 2021 A synaptic framework for the persistence of memory engrams. *Front. Synaptic Neurosci.* **13**, 661476. (doi:10.3389/fnsyn.2021.661476)
- Ebbinghaus H. 1885 *Über Das Gedächtnis: untersuchungen zur experimentellen psychologie*. Leipzig, Germany: Veit & Co.
- Ruger HA, Bussenius CE. 1913 *Memory: a contribution to experimental psychology, Hermann Ebbinghaus (1885)*. New York, NY: Teachers College, Columbia University.

31. Fields RD. 2005 Making memories stick. *Sci. Am.* **292**, 75–81. <https://www.jstor.org/stable/26060881>
32. Smolen P, Zhang Y, Byrne JH. 2016 The right time to learn: mechanisms and optimization of spaced learning. *Nat. Rev. Neurosci.* **17**, 77–88. (doi:10.1038/nrn.2015.18)
33. Bliss TV, Collingridge GL. 1993 A synaptic model of memory: long-term potentiation in the hippocampus. *Nature* **361**, 31–39. (doi:10.1038/361031a0)
34. Yuste R, Bonhoeffer T. 2001 Morphological changes in dendritic spines associated with long-term synaptic plasticity. *Annu. Rev. Neurosci.* **24**, 1071–1089. (doi:10.1146/annurev.neuro.24.1.1071)
35. Bourne JN, Harris KM. 2008 Balancing structure and function at hippocampal dendritic spines. *Annu. Rev. Neurosci.* **31**, 47–67. (doi:10.1146/annurev.neuro.31.060407.125646)
36. Kessels HW, Malinow R. 2009 Synaptic AMPA receptor plasticity and behavior. *Neuron* **61**, 340–350. (doi:10.1016/j.neuron.2009.01.015)
37. Diering GH, Huganir RL. 2018 The AMPA receptor code of synaptic plasticity. *Neuron* **100**, 314–329. (doi:10.1016/j.neuron.2018.10.018)
38. Huganir RL, Nicoll RA. 2013 AMPARs and synaptic plasticity: the last 25 years. *Neuron* **80**, 704–717. (doi:10.1016/j.neuron.2013.10.025)
39. Choquet D, Opazo P. 2022 The role of AMPAR lateral diffusion in memory. *Semin. Cell Dev. Biol.* **125**, 76–83. (doi:10.1016/j.semcdb.2022.01.009)
40. Bolton MM, Blanpied TA, Ehlers MD. 2000 Localization and stabilization of ionotropic glutamate receptors at synapses. *Cell. Mol. Life Sci.* **57**, 1517–1525. (doi:10.1007/pl00000636)
41. Turrigiano G. 2012 Homeostatic synaptic plasticity: local and global mechanisms for stabilizing neuronal function. *Cold Spring Harb. Perspect. Biol.* **4**, a005736. (doi:10.1101/cshperspect.a005736)
42. Turrigiano GG. 2000 AMPA receptors unbound: membrane cycling and synaptic plasticity. *Neuron* **26**, 5–8. (doi:10.1016/s0896-6273(00)81131-9)
43. Lisman J, Raghavachari S. 2006 A unified model of the presynaptic and postsynaptic changes during LTP at CA1 synapses. *Sci. STKE* **2006**, re11. (doi:10.1126/stke.3562006re11)
44. Opazo P, Sainlos M, Choquet D. 2012 Regulation of AMPA receptor surface diffusion by PSD-95 slots. *Curr. Opin. Neurobiol.* **22**, 453–460. (doi:10.1016/j.conb.2011.10.010)
45. Lisman J. 2017 Glutamatergic synapses are structurally and biochemically complex because of multiple plasticity processes: long-term potentiation, long-term depression, short-term potentiation and scaling. *Phil. Trans. R. Soc. B* **372**, 20160260. (doi:10.1098/rstb.2016.0260)
46. Nair D, Hossy E, Petersen JD, Constals A, Giannone G, Choquet D, Sibarita JB. 2013 Super-resolution imaging reveals that AMPA receptors inside synapses are dynamically organized in nanodomains regulated by PSD95. *J. Neurosci.* **33**, 13204–13224. (doi:10.1523/JNEUROSCI.2381-12.2013)
47. MacGillavry HD, Song Y, Raghavachari S, Blanpied TA. 2013 Nanoscale scaffolding domains within the postsynaptic density concentrate synaptic AMPA receptors. *Neuron* **78**, 615–622. (doi:10.1016/j.neuron.2013.03.009)
48. Fukata Y, Dimitrov A, Boncompain G, Vielemeyer O, Perez F, Fukata M. 2013 Local palmitoylation cycles define activity-regulated postsynaptic subdomains. *J. Cell Biol.* **202**, 145–161. (doi:10.1083/jcb.201302071)
49. Cao G, Harris KM. 2014 Augmenting saturated LTP by broadly spaced episodes of theta-burst stimulation in hippocampal area CA1 of adult rats and mice. *J. Neurophysiol.* **112**, 1916–1924. (doi:10.1152/jn.00297.2014)
50. Bell ME, Bourne JN, Chirillo MA, Mendenhall JM, Kuwajima M, Harris KM. 2014 Dynamics of nascent and active zone ultrastructure as synapses enlarge during long-term potentiation in mature hippocampus. *J. Comp. Neurol.* **522**, 3861–3884. (doi:10.1002/cne.23646)
51. Gall CM, Le AA, Lynch G. 2023 Sex differences in synaptic plasticity underlying learning. *J. Neurosci. Res.* **101**, 764–782. (doi:10.1002/jnr.24844)
52. Lynch G, Kramár EA, Babayan AH, Rumbaugh G, Gall CM. 2013 Differences between synaptic plasticity thresholds result in new timing rules for maximizing long-term potentiation. *Neuropharmacology* **64**, 27–36. (doi:10.1016/j.neuropharm.2012.07.006)
53. Kramár EA, Babayan AH, Gavin CF, Cox CD, Jafari M, Gall CM, Rumbaugh G, Lynch G. 2012 Synaptic evidence for the efficacy of spaced learning. *Proc. Natl Acad. Sci. USA* **109**, 5121–5126. (doi:10.1073/pnas.1120700109)
54. Chirillo MA, Waters MS, Lindsey LF, Bourne JN, Harris KM. 2019 Local resources of polyribosomes and SER promote synapse enlargement and spine clustering after long-term potentiation in adult rat hippocampus. *Sci. Rep.* **9**, 3861. (doi:10.1038/s41598-019-40520-x)
55. Connor SA, Siddiqui TJ. 2023 Synapse organizers as molecular codes for synaptic plasticity. *Trends Neurosci.* **46**, 971–985. (doi:10.1016/j.tins.2023.08.001)
56. Hosokawa T *et al.* 2021 CaMKII activation persistently segregates postsynaptic proteins via liquid phase separation. *Nat. Neurosci.* **24**, 777–785. (doi:10.1038/s41593-021-00843-3)
57. Chen H, Tang AH, Blanpied TA. 2018 Subsynaptic spatial organization as a regulator of synaptic strength and plasticity. *Curr. Opin. Neurobiol.* **51**, 147–153. (doi:10.1016/j.conb.2018.05.004)
58. Zhai R *et al.* 2000 Temporal appearance of the presynaptic cytomatrix protein bassoon during synaptogenesis. *Mol. Cell. Neurosci.* **15**, 417–428. (doi:10.1006/mcne.2000.0839)
59. Zhai RG, Vardinon-Friedman H, Cases-Langhoff C, Becker B, Gundelfinger ED, Ziv NE, Garner CC. 2001 Assembling the presynaptic active zone: a characterization of an active one precursor vesicle. *Neuron* **29**, 131–143. (doi:10.1016/s0896-6273(01)00185-4)
60. Jung JH, Kirk LM, Bourne JN, Harris KM. 2021 Shortened tethering filaments stabilize presynaptic vesicles in support of elevated release probability during LTP in rat hippocampus. *Proc. Natl Acad. Sci. USA* **118**, e2018653118. (doi:10.1073/pnas.2018653118)
61. Neher E, Brose N. 2018 Dynamically primed synaptic vesicle states: key to understand synaptic short-term plasticity. *Neuron* **100**, 1283–1291. (doi:10.1016/j.neuron.2018.11.024)
62. Haas KT *et al.* 2018 Pre-post synaptic alignment through neuroligin-1 tunes synaptic transmission efficiency. *eLife* **7**, e31755. (doi:10.7554/eLife.31755)
63. Franks KM, Bartol TM, Sejnowski TJ. 2002 A Monte Carlo model reveals independent signaling at central glutamatergic synapses. *Biophys. J.* **83**, 2333–2348. (doi:10.1016/S0006-3495(02)75248-X)
64. Coggan JS, Bartol TM, Esquenazi E, Stiles JR, Lamont S, Martone ME, Berg DK, Ellisman MH, Sejnowski TJ. 2005 Evidence for ectopic neurotransmission at a neuronal synapse. *Science* **309**, 446–451. (doi:10.1126/science.1108239)
65. Nadkarni S, Bartol TM, Sejnowski TJ, Levine H. 2010 Modelling vesicular release at hippocampal synapses. *PLoS Comput. Biol.* **6**, e1000983. (doi:10.1371/journal.pcbi.1000983)
66. Nadkarni S, Bartol TM, Stevens CF, Sejnowski TJ, Levine H. 2012 Short-term plasticity constrains spatial organization of a hippocampal presynaptic terminal. *Proc. Natl Acad. Sci. USA* **109**, 14 657–14 662. (doi:10.1073/pnas.1211971109)
67. Bartol TM, Land BR, Salpeter EE, Salpeter MM. 1991 Monte Carlo simulation of miniature endplate current generation in the vertebrate neuromuscular junction. *Biophys. J.* **59**, 1290–1307. (doi:10.1016/S0006-3495(91)82344-X)
68. Stiles JR, Van Helden D, Bartol TM, Salpeter EE, Salpeter MM. 1996 Miniature endplate current rise times less than 100 microseconds from improved dual recordings can be modeled with passive acetylcholine diffusion from a synaptic vesicle. *Proc. Natl Acad. Sci. USA* **93**, 5747–5752. (doi:10.1073/pnas.93.12.5747)
69. Bartol TM, Keller DX, Kinney JP, Bajaj CL, Harris KM, Sejnowski TJ, Kennedy MB. 2015 Computational reconstitution of spine calcium transients from individual proteins. *Front. Synaptic Neurosci.* **7**, 17. (doi:10.3389/fnsyn.2015.00017)
70. Franks KM, Stevens CF, Sejnowski TJ. 2003 Independent sources of quantal variability at single glutamatergic synapses. *J. Neurosci.* **23**, 3186–3195. (doi:10.1523/JNEUROSCI.23-08-03186.2003)
71. Haas KT *et al.* 2020 Correction: pre-post synaptic alignment through neuroligin-1 tunes synaptic transmission efficiency. *eLife* **9**, e65689. (doi:10.7554/eLife.65689)

72. Gonçalves J *et al.* 2020 Nanoscale co-organization and coactivation of AMPAR, NMDAR, and mGluR at excitatory synapses. *Proc. Natl Acad. Sci. USA* **117**, 14 503–14 511. (doi:10.1073/pnas.1922563117)
73. Sokolov MV, Rossokhin AV, Astrelin AV, Frey JU, Voronin LL. 2002 Quantal analysis suggests strong involvement of presynaptic mechanisms during the initial 3 h maintenance of long-term potentiation in rat hippocampal CA1 area in vitro. *Brain Res.* **957**, 61–75. (doi:10.1016/s0006-8993(02)03600-4)
74. Schulz PE, Cook EP, Johnston D. 1995 Using paired-pulse facilitation to probe the mechanisms for long-term potentiation (LTP). *J. Physiol. Paris* **89**, 3–9. (doi:10.1016/0928-4257(96)80546-8)
75. Schulz PE, Cook EP, Johnston D. 1994 Changes in paired-pulse facilitation suggest presynaptic involvement in long-term potentiation. *J. Neurosci.* **14**, 5325–5337. (doi:10.1523/JNEUROSCI.14-09-05325.1994)
76. Bosch M, Castro J, Saneyoshi T, Matsuno H, Sur M, Hayashi Y. 2014 Structural and molecular remodeling of dendritic spine substructures during long-term potentiation. *Neuron* **82**, 444–459. (doi:10.1016/j.neuron.2014.03.021)
77. Sun Y, Smirnov M, Kamasawa N, Yasuda R. 2021 Rapid ultrastructural changes in the PSD and surrounding membrane after induction of structural LTP in single dendritic spines. *J. Neurosci.* **41**, 7003–7014. (doi:10.1523/JNEUROSCI.1964-20.2021)
78. Cane M, Maco B, Knott G, Holtmaat A. 2014 The relationship between PSD-95 clustering and spine stability *in vivo*. *J. Neurosci.* **34**, 2075–2086. (doi:10.1523/JNEUROSCI.3353-13.2014)
79. Dosemeci A, Tao-Cheng JH, Vinade L, Winters CA, Pozzo-Miller L, Reese TS. 2001 Glutamate-induced transient modification of the postsynaptic density. *Proc. Natl Acad. Sci. USA* **98**, 10 428–10 432. (doi:10.1073/pnas.181336998)
80. Araki Y *et al.* 2023 Syngap regulates synaptic plasticity and cognition independent of its catalytic activity. *bioRxiv*. (doi:10.1101/2023.08.06.552111)
81. Spacek J, Harris KM. 1998 Three-dimensional organization of cell adhesion junctions at synapses and dendritic spines in area CA1 of the rat hippocampus. *J. Comp. Neurol.* **393**, 58–68. (doi:10.1002/(sici)1096-9861(19980330)393:1<58::aid-cne6>3.0.co;2-p)
82. Fannon AM, Colman DR. 1996 A model for central synaptic junctional complex formation based on the differential adhesive specificities of the cadherins. *Neuron* **17**, 423–434. (doi:10.1016/s0896-6273(00)80175-0)
83. Uchida N, Honjo Y, Johnson KR, Wheelock MJ, Takeichi M. 1996 The catenin/cadherin adhesion system is localized in synaptic junctions bordering transmitter release zones. *J. Cell Biol.* **135**, 767–779. (doi:10.1083/jcb.135.3.767)
84. Murase S, Mosser E, Schuman EM. 2002 Depolarization drives β -catenin into neuronal spines promoting changes in synaptic structure and function. *Neuron* **35**, 91–105. (doi:10.1016/s0896-6273(02)00764-x)
85. Murase S, Schuman EM. 1999 The role of cell adhesion molecules in synaptic plasticity and memory. *Curr. Opin. Cell Biol.* **11**, 549–553. (doi:10.1016/s0955-0674(99)00019-8)
86. Kasai H, Ucar H, Morimoto Y, Eto F, Okazaki H. 2023 Mechanical transmission at spine synapses: short-term potentiation and working memory. *Curr. Opin. Neurobiol.* **80**, 102706. (doi:10.1016/j.conb.2023.102706)
87. Kasai H. 2023 Unraveling the mysteries of dendritic spine dynamics: five key principles shaping memory and cognition. *Proc. Jpn. Acad., Ser. B, Phys. Biol. Sci.* **99**, 254–305. (doi:10.2183/pjab.99.018)
88. Choquet D, Triller A. 2003 The role of receptor diffusion in the organization of the postsynaptic membrane. *Nat. Rev. Neurosci.* **4**, 251–265. (doi:10.1038/nm1077)
89. Opazo P, Choquet D. 2011 A three-step model for the synaptic recruitment of AMPA receptors. *Mol. Cell. Neurosci.* **46**, 1–8. (doi:10.1016/j.mcn.2010.08.014)
90. Lu J, Helton TD, Blanpied TA, Rác B, Newpher TM, Weinberg RJ, Ehlers MD. 2007 Postsynaptic positioning of endocytic zones and AMPA receptor cycling by physical coupling of dynamin-3 to Homer. *Neuron* **55**, 874–889. (doi:10.1016/j.neuron.2007.06.041)
91. Tang AH, Chen H, Li TP, Metzbower SR, MacGillavry HD, Blanpied TA. 2016 A trans-synaptic nanocolumn aligns neurotransmitter release to receptors. *Nature* **536**, 210–214. (doi:10.1038/nature19058)
92. Pierce JP, Mayer T, McCarthy JB. 2001 Evidence for a satellite secretory pathway in neuronal dendritic spines. *Curr. Biol.* **11**, 351–355. (doi:10.1016/s0960-9822(01)00077-x)
93. Harris KM, Weinberg RJ. 2012 Ultrastructure of synapses in the mammalian brain. *Cold Spring Harb. Perspect. Biol.* **4**, a005587. (doi:10.1101/cshperspect.a005587)
94. Ehlers MD. 2013 Dendritic trafficking for neuronal growth and plasticity. *Biochem. Soc. Trans.* **41**, 1365–1382. (doi:10.1042/BST20130081)
95. Spacek J, Harris KM. 1997 Three-dimensional organization of smooth endoplasmic reticulum in hippocampal CA1 dendrites and dendritic spines of the immature and mature rat. *J. Neurosci.* **17**, 190–203. (doi:10.1523/JNEUROSCI.17-01-00190.1997)
96. Cooney JR, Hurlburt JL, Selig DK, Harris KM, Fiala JC. 2002 Endosomal compartments serve multiple hippocampal dendritic spines from a widespread rather than a local store of recycling membrane. *J. Neurosci.* **22**, 2215–2224. (doi:10.1523/JNEUROSCI.22-06-02215.2002)
97. Knowles RB, Sabry JH, Martone ME, Deerinck TJ, Ellisman MH, Bassell GJ, Kosik KS. 1996 Translocation of RNA granules in living neurons. *J. Neurosci.* **16**, 7812–7820. (doi:10.1523/JNEUROSCI.16-24-07812.1996)
98. Krichevsky AM, Kosik KS. 2001 Neuronal RNA granules: a link between RNA localization and stimulation-dependent translation. *Neuron* **32**, 683–696. (doi:10.1016/s0896-6273(01)00508-6)
99. Wells DG, Dong X, Quinlan EM, Huang YS, Bear MF, Richter JD, Fallon JR. 2001 A role for the cytoplasmic polyadenylation element in NMDA receptor-regulated mRNA translation in neurons. *J. Neurosci.* **21**, 9541–9548. (doi:10.1523/JNEUROSCI.21-24-09541.2001)
100. Wu L *et al.* 1998 CPEB-mediated cytoplasmic polyadenylation and the regulation of experience-dependent translation of α -CaMKII mRNA at synapses. *Neuron* **21**, 1129–1139. (doi:10.1016/s0896-6273(00)80630-3)
101. Steward O, Schuman EM. 2003 Compartmentalized synthesis and degradation of proteins in neurons. *Neuron* **40**, 347–359. (doi:10.1016/s0896-6273(03)00635-4)
102. Sun C, Nold A, Fusco CM, Rangaraju V, Tchumatchenko T, Heilemann M, Schuman EM. 2021 The prevalence and specificity of local protein synthesis during neuronal synaptic plasticity. *Sci. Adv.* **7**, eabj0790. (doi:10.1126/sciadv.abj0790)
103. Ostroff LE, Cain CK. 2022 Persistent up-regulation of polyribosomes at synapses during long-term memory, reconsolidation, and extinction of associative memory. *Learn. Mem.* **29**, 192–202. (doi:10.1101/lm.053577.122)
104. Martin KC, Casadio A, Zhu H, E Y, Rose JC, Chen M, Bailey CH, Kandel ER. 1997 Synapse-specific, long-term facilitation of aplysia sensory to motor synapses: a function for local protein synthesis in memory storage. *Cell* **91**, 927–938. (doi:10.1016/S0092-8674(00)80484-5)
105. Huang YS, Mendez R, Fernandez M, Richter JD. 2023 CPEB and translational control by cytoplasmic polyadenylation: impact on synaptic plasticity, learning, and memory. *Mol. Psychiatry* **28**, 2728–2736. (doi:10.1038/s41380-023-02088-x)
106. Ostroff LE, Watson DJ, Cao G, Parker PH, Smith H, Harris KM. 2018 Shifting patterns of polyribosome accumulation at synapses over the course of hippocampal long-term potentiation. *Hippocampus* **28**, 416–430. (doi:10.1002/hipo.22841)
107. Bear MF. 1995 Mechanism for a sliding synaptic modification threshold. *Neuron* **15**, 1–4. (doi:10.1016/0896-6273(95)90056-x)

108. Bienenstock EL, Cooper LN, Munro PW. 1982 Theory for the development of neuron selectivity: orientation specificity and binocular interaction in visual cortex. *J. Neurosci* **2**, 32–48. (doi:10.1523/JNEUROSCI.02-01-00032.1982)
109. Abraham WC, Mason-Parker SE, Bear MF, Webb S, Tate WP. 2001 Heterosynaptic metaplasticity in the hippocampus *in vivo*: a BCM-like modifiable threshold for LTP. *Proc. Natl Acad. Sci. USA* **98**, 10 924–10 929. (doi:10.1073/pnas.181342098)
110. Govindarajan A, Kelleher RJ, Tonegawa S. 2006 A clustered plasticity model of long-term memory engrams. *Nat. Rev. Neurosci.* **7**, 575–583. (doi:10.1038/nrn1937)
111. De Roo M, Klauser P, Muller D. 2008 LTP promotes a selective long-term stabilization and clustering of dendritic spines. *PLoS Biol.* **6**, e219. (doi:10.1371/journal.pbio.0060219)
112. Pulikkottil VV, Somashekar BP, Bhalla US. 2021 Computation, wiring, and plasticity in synaptic clusters. *Curr. Opin. Neurobiol.* **70**, 101–112. (doi:10.1016/j.conb.2021.08.001)
113. Kantor DB, Lanzrein M, Stary SJ, Sandoval GM, Smith WB, Sullivan BM, Davidson N, Schuman EM. 1996 A role for endothelial NO synthase in LTP revealed by adenovirus-mediated inhibition and rescue. *Science* **274**, 1744–1748. (doi:10.1126/science.274.5293.1744)
114. Schuman EM, Meffert MK, Schulman H, Madison DV. 1994 An ADP-ribosyltransferase as a potential target for nitric oxide action in hippocampal long-term potentiation. *Proc. Natl Acad. Sci. USA* **91**, 11 958–11 962. (doi:10.1073/pnas.91.25.11958)
115. Schuman EM, Madison DV. 1991 A requirement for the intercellular messenger nitric oxide in long-term potentiation. *Science* **254**, 1503–1506. (doi:10.1126/science.1720572)
116. Kastellakis G, Cai DJ, Mednick SC, Silva AJ, Poirazi P. 2015 Synaptic clustering within dendrites: an emerging theory of memory formation. *Prog. Neurobiol.* **126**, 19–35. (doi:10.1016/j.pneurobio.2014.12.002)
117. Poirazi P, Mel BW. 2001 Impact of active dendrites and structural plasticity on the memory capacity of neural tissue. *Neuron* **29**, 779–796. (doi:10.1016/S0896-6273(01)00252-5)
118. Gasparini S, Losonczy A, Chen X, Johnston D, Magee JC. 2007 Associative pairing enhances action potential back-propagation in radial oblique branches of CA1 pyramidal neurons. *J. Physiol.* **580**, 787–800. (doi:10.1113/jphysiol.2006.121343)
119. Losonczy A, Makara JK, Magee JC. 2008 Compartmentalized dendritic plasticity and input feature storage in neurons. *Nature* **452**, 436–441. (doi:10.1038/nature06725)
120. Branco T, Häusser M. 2010 The single dendritic branch as a fundamental functional unit in the nervous system. *Curr. Opin. Neurobiol.* **20**, 494–502. (doi:10.1016/j.conb.2010.07.009)
121. Larkum ME, Nevian T. 2008 Synaptic clustering by dendritic signalling mechanisms. *Curr. Opin. Neurobiol.* **18**, 321–331. (doi:10.1016/j.conb.2008.08.013)
122. Madison DV, Schuman EM. 1995 Diffusible messengers and intercellular signaling: locally distributed synaptic potentiation in the hippocampus. *Curr. Top. Microbiol. Immunol.* **196**, 5–6. (doi:10.1007/978-3-642-79130-7_2)
123. Garthwaite J. 2018 Nitric oxide as a multimodal brain transmitter. *Brain Neurosci. Adv.* **2**, 239821281881068. (doi:10.1177/2398212818810683)
124. Hawkins RD, Zhuo M, Arancio O. 1994 Nitric oxide and carbon monoxide as possible retrograde messengers in hippocampal long-term potentiation. *J. Neurobiol.* **25**, 652–665. (doi:10.1002/neu.480250607)
125. Anastassiou CA, Koch C. 2015 Ephaptic coupling to endogenous electric field activity: why bother? *Curr. Opin. Neurobiol.* **31**, 95–103. (doi:10.1016/j.conb.2014.09.002)
126. Timofeev I, Bazhenov M, Seigneur J, Sejnowski T. 2010 Neocortical synchronization. *Epilepsia* **51**, 18. (doi:10.1111/j.1528-1167.2010.02804.x)
127. Frank AC *et al.* 2018 Hotspots of dendritic spine turnover facilitate clustered spine addition and learning and memory. *Nat. Commun.* **9**, 422. (doi:10.1038/s41467-017-02751-2)
128. Hedrick NG *et al.* 2022 Learning binds new inputs into functional synaptic clusters via spinogenesis. *Nat. Neurosci.* **25**, 726–737. (doi:10.1038/s41593-022-01086-6)
129. Harris KM. 1995 How multiple-synapse boutons could preserve input specificity during an interneuronal spread of LTP. *Trends Neurosci.* **18**, 365–369. (doi:10.1016/0166-2236(95)93930-V)
130. Choi DI, Kaang BK. 2022 Interrogating structural plasticity among synaptic engrams. *Curr. Opin. Neurobiol.* **75**, 102552. (doi:10.1016/j.conb.2022.102552)
131. Ortega-de San Luis C, Ryan TJ. 2022 Understanding the physical basis of memory: molecular mechanisms of the engram. *J. Biol. Chem.* **298**, 101866. (doi:10.1016/j.jbc.2022.101866)
132. Han DH, Park P, Choi DI, Bliss TVP, Kaang BK. 2022 The essence of the engram: cellular or synaptic? *Semin. Cell Dev. Biol.* **125**, 122–135. (doi:10.1016/j.semdb.2021.05.033)
133. Gall CM, Le AA, Lynch G. 2023 Sex differences in synaptic plasticity underlying learning. *J. Neurosci. Res.* **101**, 764–782. (doi:10.1002/jnr.24844)
134. Lisman J. 2017 Criteria for identifying the molecular basis of the engram (CaMKII, PKMzeta). *Mol. Brain* **10**, 55. (doi:10.1186/s13041-017-0337-4)
135. Parvez S, Ramachandran B, Frey JU. 2010 Properties of subsequent induction of long-term potentiation and/or depression in one synaptic input in apical dendrites of hippocampal CA1 neurons *in vitro*. *Neuroscience* **171**, 712–720. (doi:10.1016/j.neuroscience.2010.09.018)
136. Oh WC, Hill TC, Zito K. 2013 Synapse-specific and size-dependent mechanisms of spine structural plasticity accompanying synaptic weakening. *Proc. Natl Acad. Sci. USA* **110**, E305–E312. (doi:10.1073/pnas.1214705110)
137. Mulkey RM, Malenka RC. 1992 Mechanisms underlying induction of homosynaptic long-term depression in area CA1 of the hippocampus. *Neuron* **9**, 967–975. (doi:10.1016/0896-6273(92)90248-c)
138. Jang J, Anisimova M, Oh WC, Zito K. 2021 Induction of input-specific spine shrinkage on dendrites of rodent hippocampal CA1 neurons using two-photon glutamate uncaging. *STAR Protoc.* **2**, 100996. (doi:10.1016/j.xpro.2021.100996)
139. Malenka RC. 2003 Synaptic plasticity and AMPA receptor trafficking. *Ann. N. Y. Acad. Sci.* **1003**, 1–11. (doi:10.1196/annals.1300.001)
140. Chen Y, Wang X, Xiao B, Luo Z, Long H. 2023 Mechanisms and functions of activity-regulated cytoskeleton-associated protein in synaptic plasticity. *Mol. Neurobiol.* **60**, 5738–5754. (doi:10.1007/s12035-023-03442-4)
141. Parkinson GT, Hanley JG. 2018 Mechanisms of AMPA receptor endosomal sorting. *Front. Mol. Neurosci.* **11**, 440. (doi:10.3389/fnmol.2018.00440)
142. Compans B *et al.* 2021 NMDAR-dependent long-term depression is associated with increased short term plasticity through autophagy mediated loss of PSD-95. *Nat. Commun.* **12**, 2849. (doi:10.1038/s41467-021-23133-9)
143. Rosendale M, Jullié D, Choquet D, Perrais D. 2017 Spatial and temporal regulation of receptor endocytosis in neuronal dendrites revealed by imaging of single vesicle formation. *Cell Rep.* **18**, 1840–1847. (doi:10.1016/j.celrep.2017.01.081)
144. Pougnet JT, Compans B, Martinez A, Choquet D, Hosy E, Boué-Grabot E. 2016 P2X-mediated AMPA receptor internalization and synaptic depression is controlled by two CaMKII phosphorylation sites on GluA1 in hippocampal neurons. *Sci. Rep.* **6**, 31836. (doi:10.1038/srep31836)
145. Bastrikova N, Gardner GA, Reece JM, Jeromin A, Dudek SM. 2008 Synapse elimination accompanies functional plasticity in hippocampal neurons. *Proc. Natl Acad. Sci. USA* **105**, 3123–3127. (doi:10.1073/pnas.0800027105)